Validation of ASTM F1264 models in Alfonso™: Four-point bending of titanium humeral nail

Non-Confidential Technical Whitepaper – 12 May 2023

Experiments and Analysis: Janice Oentaryo, PhD; Rezaul Tharim; Sloan Kulper, PhD; and Erica Ueda Boles, PhD
Visualizations: Abbas Alvi and Eka Tjong

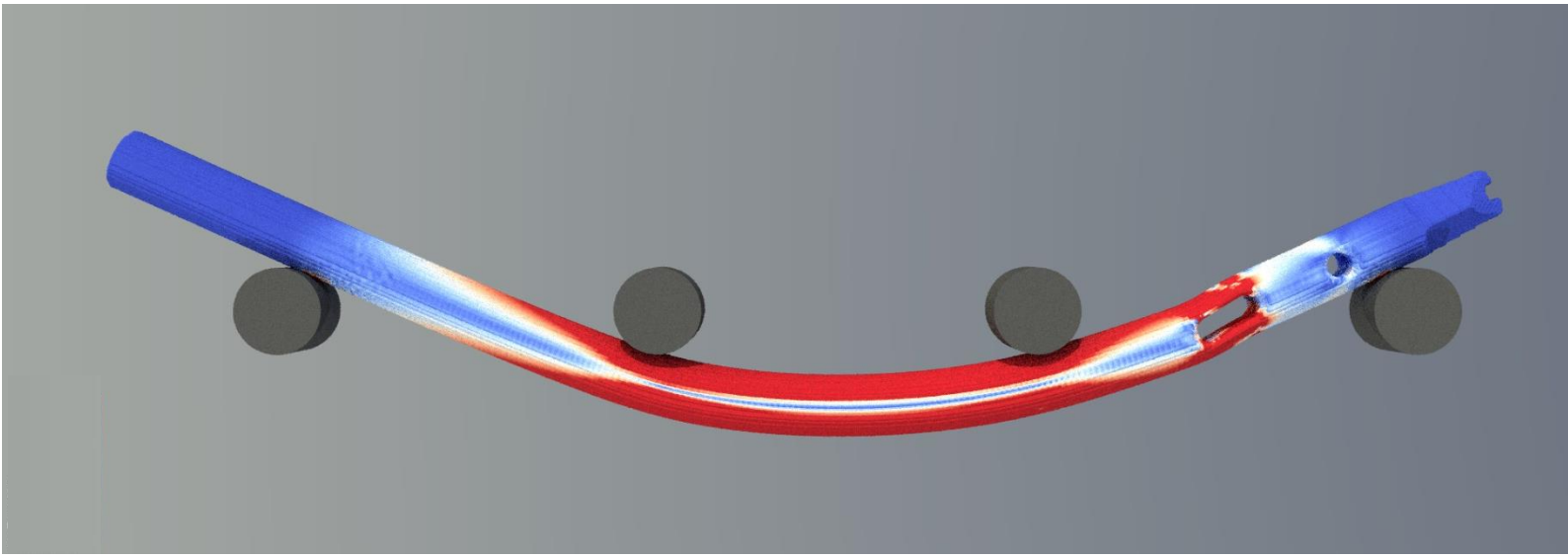

Abstract

A computational model of the ASTM F1264-16 $^{\varepsilon 1}$ A1 static four-point bending test for a Ti-6Al-4V ELI (e.g., material per ASTM F136-13-2021) humeral intramedullary nail (Ø10/8 mm, L260 mm, Ø3 mm cannulation) was built using the *Alfonso*™ particle-based simulation system and validated via comparison to experimental data. The titanium humeral nail (n = 5) was tested by an independent laboratory according to the ASTM F1264-16 $^{\varepsilon 1}$ A1 standard. Devices were axially compressed at a loading rate of 0.1 mm/s until implant failure or until the maximum load capacity of the test frame was reached. The three-dimensional model of the nail was converted to a particle model in *Alfonso*™ at a resolution of 200 µm/particle and simulation of the ASTM F1264-16 $^{\varepsilon 1}$ static four-point bending test was performed, using a material model based on the typical properties of Ti-6Al-4V ELI. In the physical test, the average yield load of the intramedullary nail was 2,505 N at an average yield displacement of 8.73 mm with an average bending stiffness of 330.86 N/mm, average bending moment to yield of 65.14 Nm, and average bending structural stiffness of 19.34 Nm^2. In the simulated test, the yield load was 2,341 N at the yield displacement of 7.98 mm with a bending stiffness of 341.65 N/mm, average bending moment to yield of 62.2 Nm, and bending structural stiffness of 20.02 Nm^2. The average CCC (concordance correlation coefficient) between the force–displacement curves for the simulation and experiment was >0.97, suggesting excellent concordance. *Alfonso*™ can accurately predict the bending strength and bending stiffness of intramedullary fixation devices given the dimensions of the test setup and standard material properties.

Background and objectives

ASTM F1264-16 $^{\varepsilon 1}$ is a standard specification and provides test methods to characterize and evaluate the design and mechanical performance of intramedullary fixation devices (IMFDs, e.g., under FDA product code HSB, 21 CFR §888.3020) designed for implantation in the medullary canal for the fixation of fractures.[1] The standard lists a battery of tests required to demonstrate that a study device is substantially equivalent to a legally marketed predicate device in a 510(k) premarket submission, which includes the ASTM F1264-16 $^{\varepsilon 1}$ A1 static four-point bend test. The static four-point bend test is intended to measure the bending strength and bending stiffness intrinsic to the design and material of the IMFD. Alfonso's particle-based model of ASTM F1264-16 $^{\varepsilon 1}$ A1 can be used to quickly predict the likelihood that a candidate design will perform sufficiently without needing to produce and test a physical prototype. To validate Alfonso's predictions, we compared the load-displacement curves of simulated and physical static four-point bend tests of titanium-6 aluminum-4 vanadium extra low interstitials (Ti-6Al-4V ELI) humeral nails.

Materials and methods

Preparation and testing of physical specimens

Humeral nails underwent physical mechanical ASTM F1264-16 $^{\varepsilon 1}$ A1 static four-point bend tests (Ti-6Al-4V ELI per ASTM F136 material specification, Ø10/8 mm, L260 mm, Ø3 mm cannulation, right humerus, n=5 samples). The physical ASTM F1264-16 $^{\varepsilon 1}$ A1 static four-point bend test was performed by an independent certified testing laboratory using the test setup illustrated in Figure 1 and Figure 2. Each intramedullary nail sample was placed onto a pair of cylindrical support rollers (Ø 12 mm) and a static compressive load was applied by a pair of cylindrical loading rollers (Ø 12 mm). The span between the support rollers (L) was 156 mm and the span between the loading rollers (c) was 52 mm. These parameters are also summarized in Table 1. These ranges of spans are within the specified values in the ASTM F1264-16 $^{\varepsilon 1}$ A1 standard (shown in Figure 1) to minimize interlaboratory variability and provide consistency with previous ASTM standards for four-point bend testing of IMFDs.

Table 1. Parameters for the ASTM F1264-16 $^{\varepsilon 1}$ A1 static four-point bend tests

Parameter	ASTM F1264
Center span (*c*): Distance between two loading rollers	52 mm
Loading span (*s*): Distance between the loading roller and the nearest support roller	52 mm
Total span (*L*): Distance between two support rollers (L = c + 2s)	156 mm
Diameter of the rollers	12 mm

In the position and orientation of the intramedullary nail with the proximal notch facing down, a distal hole and an elongated hole were included between the support rollers, as illustrated in Figure 2. The laser marking on the nail was not located between the support rollers. This device design was chosen for initial validation because the shaft, as the main part tested in the static four-point bend test, is a typical rod shape with dimensions or diameters commonly used clinically and offered by various manufacturers.[2]–[4] The material Ti-6Al-4V ELI (Grade 23) is a common choice of material for the IMFDs due to its enhanced biomechanical and biocompatible performance.[5],[6]

Material properties of Ti-6Al-4V ELI (Grade 23) as summarized from manufacturers' sources are listed in Table 2.[7]–[9] The compressive load was applied by the two cylindrical loading rollers using a hydraulic test frame at a rate of 0.1 mm/s at ambient air and room temperature conditions. Compression was applied until functional failure or until the maximum load capacity of the test frame was reached.

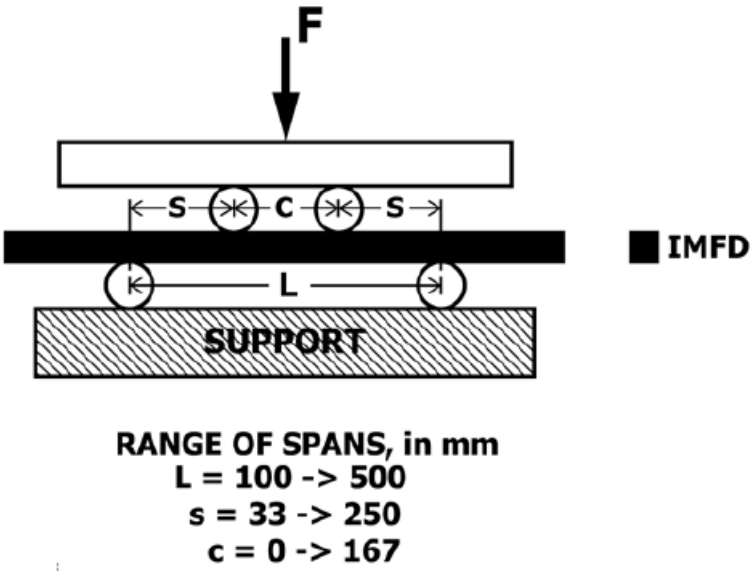

Figure 1. Static four-point bend test setup with the range of spans of the loading and support rollers specified in ASTM F1264-16 $^{\varepsilon 1}$ A1 test standard.

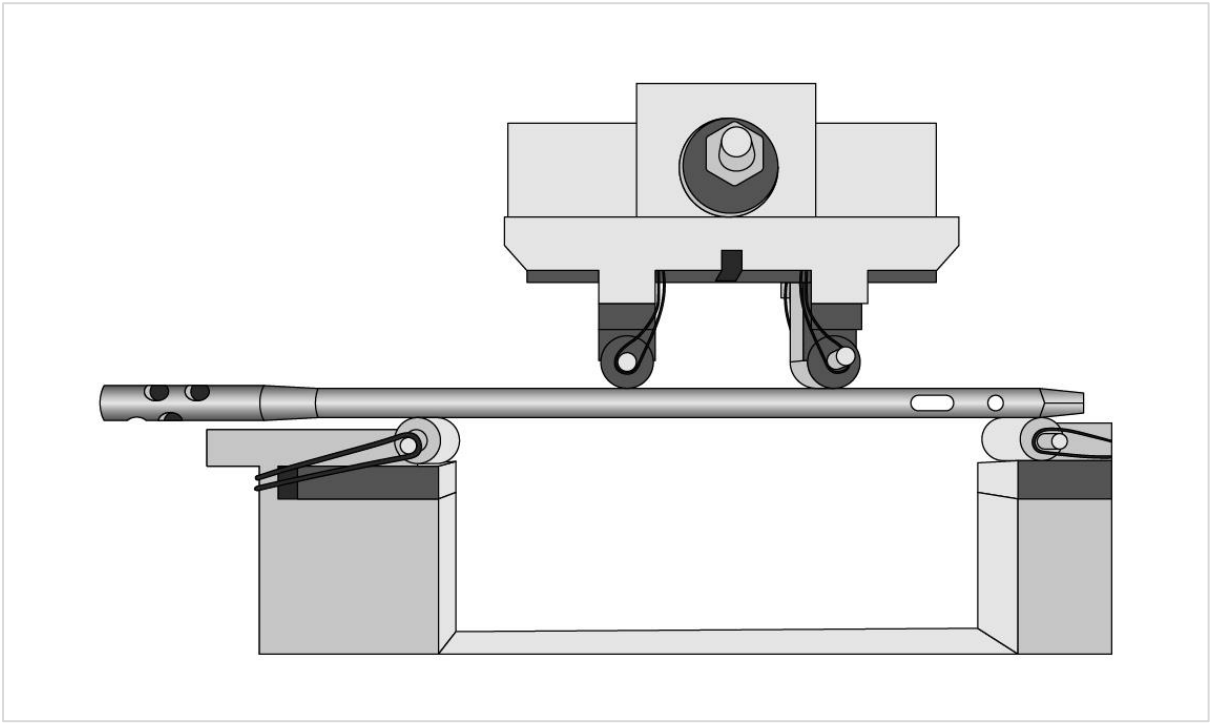

Figure 2. Diagram of the physical experimental setup used for the static four-point bending tests. Illustration by Eka Tjong

Preparation and testing of simulated specimens

A CAD model of the intramedullary nail was exported to STL format using a fine mesh (<1 µm deviation from the mathematical surface) and developed into a particle-based model in *Alfonso*™ at a resolution of 200 µm per particle (see "Appendix I: Notes on particle-based method simulation in *Alfonso*™"). The nail was modeled using standard material properties for Ti-6Al-4V ELI as summarized in Table 2. Four simulated identical Ø 12 mm rigid rollers were also exported as fine meshes and generated into particle-based models, likewise at 200 µm per particle. Components in the simulation setup (Figure 3) were arranged in the same manner as in the physical test; the loading rollers were moved downward (in the -Z direction) at a rate of 2.5 m/s. Compression continued until either simulated functional failure occurred or the simulated load exceeded the maximum capacity of the test frame used in the physical test case that served as a reference for the simulation.

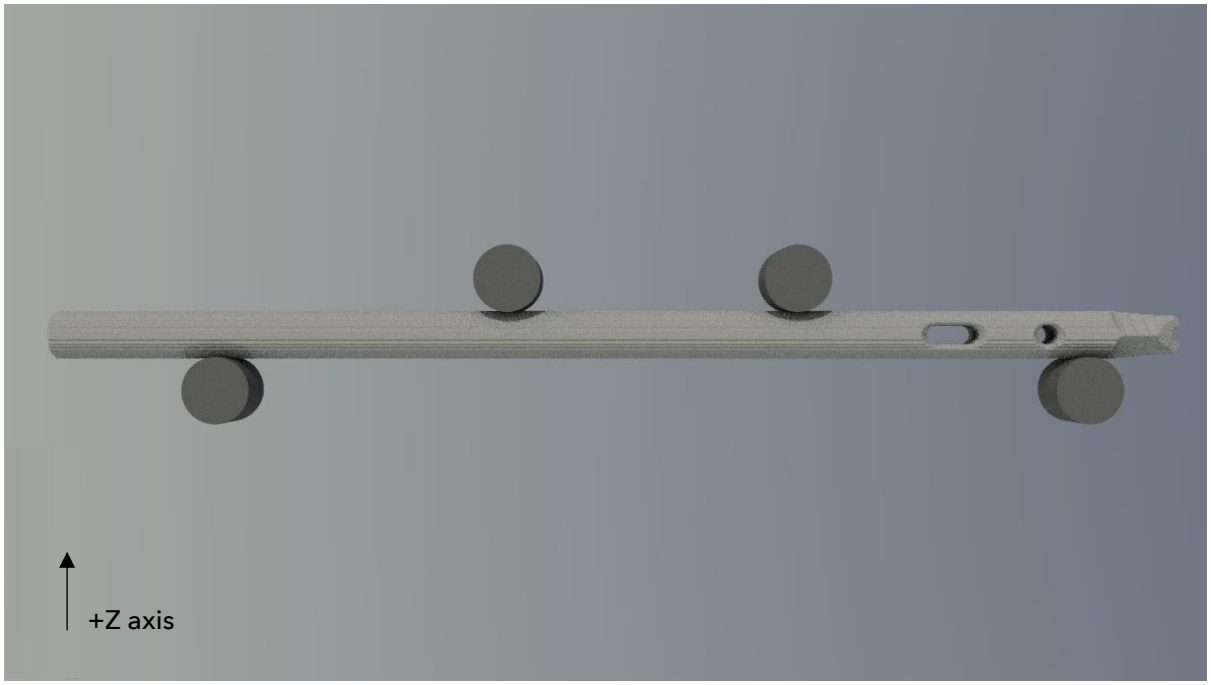

Figure 3. Simulated test setup for the static four-point bending test in Alfonso™

A sensitivity analysis was conducted to determine the maximum uniaxial compression rate (2.5 m/s), below which there was no observable change in the force–displacement curve. This rate was also much less than the calculated speed of sound of the implant material (Table 2). Deviations between the physical and simulated testing protocols and the published ASTM F1264-16$^{\varepsilon 1}$ A1 standard are summarized in Table 3. Note that models in *Alfonso*™ do not typically simulate the strain-rate dependent viscoelastic behaviors of materials for static tests; as physical static benchtop tests are usually conducted at very low rates of motion, we consider strain-rate components to be negligible. The speed of sound c was calculated to set a theoretical upper bound for the rate of motion of the simulation (Table 2), Eq.1:

$$c = \sqrt{\frac{(K_f + \frac{4}{3}G_f)}{\rho}}$$

Where K_f is the bulk modulus, G_f is the shear modulus, and ρ is the density (kg/m^3) of Ti6Al4V ELI.

Table 2. Typical material properties of Ti-6Al-4V ELI from manufacturers' datasheets [7]–[9]

Typical material properties	Ti-6Al-4V ELI (Grade 23)
Density (kg/m^3)	4428.78
Elastic Modulus (GPa)	104.80
Poisson's Ratio	0.342
0.2% Yield Strength (MPa)	827
Ultimate Tensile Strength (MPa)	896
Elongation at break (%)	15
Reduction of Area (%)	45
Speed of sound $\mathbf{c}$ (m/s)	6059

Table 3. Deviations between physical and simulated testing protocols and the published ASTM F1264-16$^{\varepsilon 1}$ A1 standard

Test Setup Procedures / Parameters		ASTM F1264-16$^{\varepsilon 1}$ A1 Static four-point bend method	Physical test	Simulation
Test setup procedures	Spans and sizes of the rollers	For long, small-diameter, solid section IMFDs, smaller rollers and spans are adequate to measure the bending of the IMFD. Meanwhile, for hollow and open-section IMFDs, long spans and large-diameter rollers will minimize local artifacts at the load and support point as much as possible. Loading rollers should be the rolling type.	Follows the ASTM F1264-16$^{\varepsilon 1}$ A1 standard to determine the spans and diameters of the rollers	Same spans and diameters of the rollers as the physical tests. Loading cylinders do not roll.
	Span between the two support rollers (L)	100 to 500 mm	156 mm	156 mm
	Span between the loading rollers (c)	No greater than L/3 Up to 167 mm	52 mm	52 mm
	Span from a load roller to the nearest support roller (s)	33 to 250 mm	52 mm	52 mm

Test Setup Procedures / Parameters		ASTM F1264-16 $^{\varepsilon 1}$ A1 Static four-point bend method	Physical test	Simulation
	Diameter of the rollers	10 to 26 mm	12 mm	12 mm
	Load application	Equal loads are applied at each of the loading points (typically, a single load centered over the load points as shown in Figure 1)	Follows the ASTM F1264-16 $^{\varepsilon 1}$ A1 standard	Follows the ASTM F1264-16 $^{\varepsilon 1}$ A1 standard
	Sample size	Usually, n=3 minimum per design	n=5 per design	n=1 per design
Parameters	Compression rate	No greater than 1 mm/s	0.1 mm/s	2.5 m/s * (See Eq.1)
	Data collection time interval	Not mentioned; suitable to continuously record load versus load fixture displacement	Not mentioned	1 x 10^{-9} s
	Type of data	Load–displacement data, which will be used to calculate the bending stiffness (N/mm) (the slope of the linear elastic region), 0.2% yield load (N), yield displacement (mm), bending moment to yield (Nm), and bending structural stiffness (Nm^2), mode of failure	Follows the ASTM F1264-16 $^{\varepsilon 1}$ A1 standard	Follows the ASTM F1264-16 $^{\varepsilon 1}$ A1 standard
	End point	Not mentioned	The load–displacement data are generated until the machine limit is reached or upon functional or mechanical failure of the intramedullary nail.	Up to the maximum displacement from the physical test
	Resolution (specific to simulation)	Not applicable	Not applicable	200 µm

Data and statistical analyses

The load–displacement data were normalized such that zero displacement was set at the lowest initial force common for both the physical data and the *Alfonso*™ simulation data. The bending stiffness (K in N/mm) is defined as the maximum slope of the linear elastic region of the load-displacement curve, which was calculated in the load range from 500 N to 1,500 N. Yield load (in N) was determined from the load–displacement curve as the applied load required to produce a permanent deformation equal to the offset displacement. Yield displacement (in mm) was determined from the load–displacement curve as the displacement when an intramedullary nail has a permanent deformation equal to the offset displacement.

The offset displacement ($Y_{0.2\%}$ in mm) is the permanent deflection at the loading point for 0.2% maximum plastic strain, where the ASTM F1264-16 $^{\varepsilon 1}$ A1 standard has specified the formula as the following (Eq.2):

$$Y_{0.2\%} = s\,(L + 2c)/(1500 D_{IMFD})$$

Where the loading span (s), total span (L), and center span (c) can be seen in Table 1 and the diameter of the IMFD (D_{IMFD}) was 8 mm, resulting in the calculated offset displacement ($Y_{0.2\%}$) of 1.13 mm.

Bending moment to yield (M_y in Nm) is calculated by estimating the load at 0.2% maximum plastic strain, where the formula is specified as the following (Eq.3):

$$M_y = 0.5\, F_y s$$

Where F_y is the yield force and s is the loading span.

Bending structural stiffness (EI_e in Nm^2) is calculated as the IMFD's resistance to bending, normalized to the cross-sectional properties of the working length, where the formula is specified as the following (Eq.4):

$$EI_e = s^2(L + 2c)(F/y)/12$$

Where the loading span (s), total span (L), and center span (c) can be seen in Table 1 and F/y is the bending stiffness (K in N/mm) determined by the slope of the linear elastic portion of the load-displacement curve.

To serve as additional quantitative analysis on the load–displacement graphs, concordance analyses were performed across the load–displacement curves to examine the extent of similarity. The numbers of data points obtained from the physical tests and *Alfonso*™ simulations varied due to the difference in data collection intervals. To directly compare and analyse the load–displacement data for the concordance analysis, Python scripts were used to resample the data sets to the same displacement values and interpolate the load values without changing the load–displacement curves' shape or magnitude. Statistical analyses were performed using MedCalc® (MedCalc Software Ltd, Ostend, Belgium).

Note: Lin's concordance correlation coefficient (CCC)

Lin's concordance correlation coefficient (CCC) evaluates the degree to which pairs of observations fall on the 45° line through the origin (i.e., the line of equality).[10], [11] The concordance correlation coefficient is calculated as $\rho_c = \rho \times C_b$ ($-1 \le \rho_c \le 1$) where:

- ρ is the Pearson correlation coefficient, which measures how far each observation deviates from the best-fit line, and is a measure of precision, and

- C_b is a bias correction factor that measures how far the best-fit line deviates from the 45° line through the origin and is a measure of accuracy ($0 < C_b \leq 1$; $C_b = 1$ when there is no deviation from the 45° line).

A CCC value of 1 indicates strong concordance, while a value of -1 indicates strong discordance. Borrowing from the standard interpretation of Pearson's correlation coefficient or intraclass correlation coefficients, we assume that positive CCC values <0.20 indicate "poor" concordance, while values >0.80 indicate "excellent" concordance.

Results

After undergoing static four-point nail bending, either physical or simulated, all samples underwent functional failure due to plastic deformation. The plastic deformation observed in the simulation is represented by the stress and material failure of the nail as shown in Figure 4.

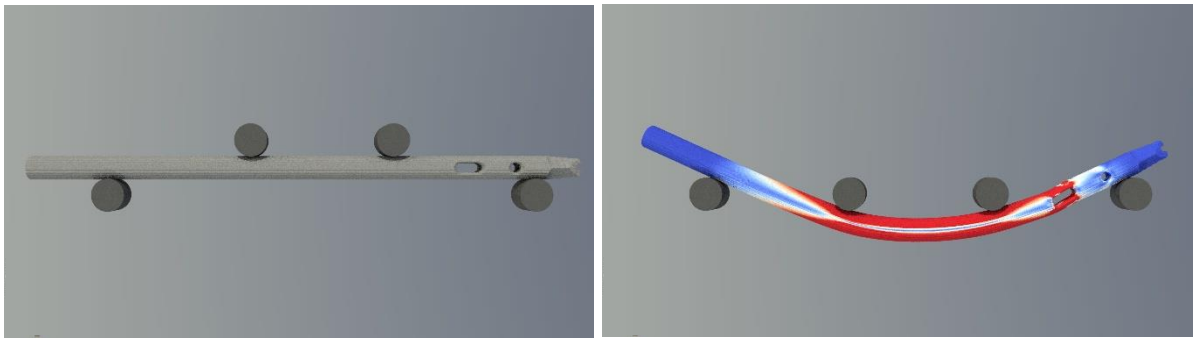

Figure 4. Representative images showing a simulated ASTM F1264-16 $^{\varepsilon 1}$ A1 static four-point nail bending test

In general, the overall load-displacement curves were comparable between the physical and simulation data, especially in the linear-elastic region that is critical for calculating the different measurement outputs (see Figure 5); the average bending stiffness, K, values were 330.86 and 341.65 N/mm in the physical and simulated tests, respectively (see Table 4). The average yield load of the intramedullary nail was 2,505 N at an average yield displacement of 8.73 mm in the physical tests, whereas the simulated test resulted in a yield load of 2,341 N at yield displacement of 7.98 mm. The average bending moment to yield values were 65.14 Nm and 62.20 Nm in the physical and simulated tests, respectively. The bending structural stiffness, EI_e, values were 19.34 N/m^2 and 20.02 Nm^2. The average CCC (concordance correlation coefficient) between the force-displacement curves for the simulation and experiment was >0.97 (using more than 325 sample points per curve, see Table 5), suggesting excellent concordance. *Alfonso*™ can accurately predict the bending strength and bending stiffness of an intramedullary fixation device given the dimensions of the test setup and standard material properties. The mode of failure in both the physical and simulated test was plastic deformation and bending of the nail shaft as well as some deformation of the elongated hole.

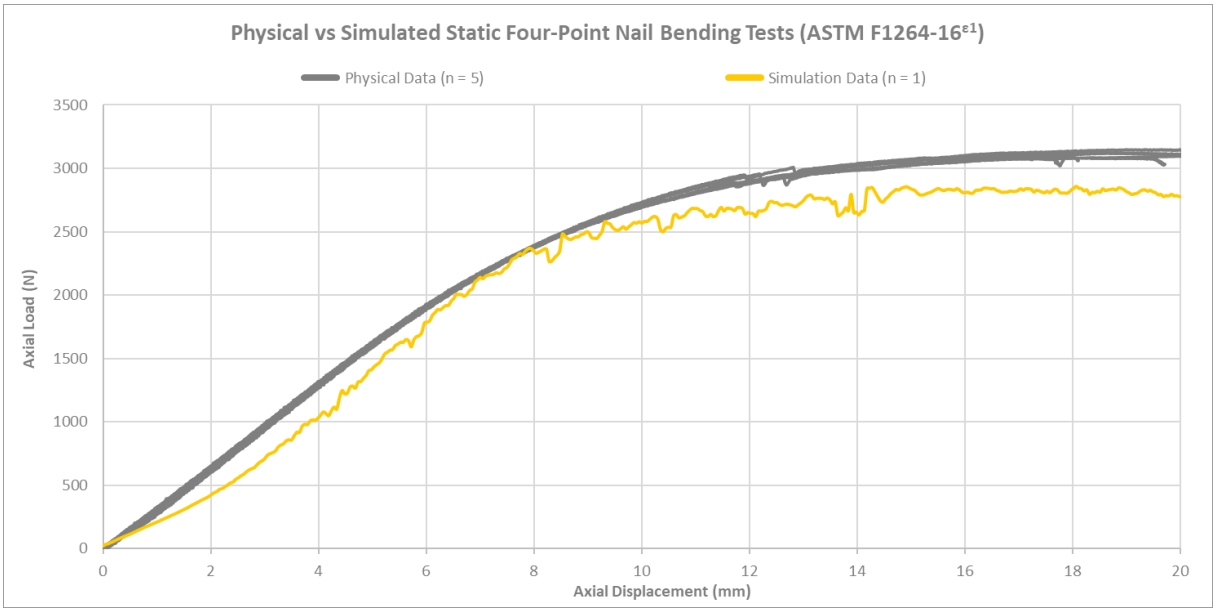

Figure 5. Load–displacement curves from the physical experiment (n = 5) and the simulated (n = 1) static four-point bending tests for a Ti-6Al-4V ELI humeral nail of Ø10/8 mm, L260 mm, Ø3 mm cannulation

Table 4. Calculated values from the physical experiment (n = 5) and the simulated (n = 1) static four-point bending tests for a Ti-6Al-4V ELI humeral nail of Ø10/8 mm, L260 mm, Ø3 mm cannulation

Specimens	Ti-6Al-4V ELI humeral nail of Ø10/8 mm L260 mm, Ø3 mm cannulation, right arm				
Physical Tests	Yield load (N)	Displacement at yield load (mm)	Bending stiffness (K, N/mm)	Bending moment to yield (M_y, Nm)	Bending structural stiffness (EI_e, N/m^2)
Specimen 1	2,473.52	8.54	333.74	64.31	19.55
Specimen 2	2,475.40	8.66	330.40	64.36	19.36
Specimen 3	2,492.95	8.71	328.62	64.82	19.25
Specimen 4	2,552.60	8.94	326.66	66.37	19.14
Specimen 5	2,532.14	8.78	330.86	65.84	19.38
Standard Deviation	35.41	0.15	2.64	0.92	0.15
Physical test Average	2,505.32	8.73	330.86	65.14	19.34
Simulated Test	2,341.68	7.98	341.65	62.20	20.02

Table 5. Concordance analysis of the load-displacement curves from ASTM F1264-16 $^{\varepsilon 1}$ A1 static four-point bending tests for a Ti-6Al-4V ELI humeral nail of Ø10/8 mm, L260 mm, Ø3 mm cannulation

Variables	Ti-6Al-4V ELI humeral nail of Ø10/8 mm L260 mm, Ø3 mm cannulation, right arm				
	Physical Data 1 vs Simulation Data	Physical Data 2 vs Simulation Data	Physical Data 3 vs Simulation Data	Physical Data 4 vs Simulation Data	Physical Data 5 vs Simulation Data
Sample size (curve data points)	405	356	393	405	362
Concordance correlation Coefficient (CCC)	0.9760	0.9812	0.9779	0.9708	0.9764
95% Confidence Interval	0.9721 to 0.9794	0.9778 to 0.9841	0.9742 to 0.9811	0.9661 to 0.9749	0.9722 to 0.9799
Pearson correlation coefficient, ρ (precision)	0.9960	0.9964	0.9964	0.9958	0.9961
Bias correction factor, C_b (accuracy)	0.9799	0.9848	0.9814	0.9749	0.9801

Conclusion

This validation study suggests that *Alfonso*™ can accurately predict the bending strength and bending stiffness of a Ti-6Al-4V ELI Ø10/8 mm humeral intramedullary nail in a static four-point bending test, providing supplementary data or replacing certain physical testing according to ASTM F1264-16 $^{\varepsilon 1}$ "Standard Specification and Test Methods for Intramedullary Fixation Devices." The measurement outputs from the *Alfonso*™ simulations of the static four-point bending test follow the ASTM F1264-16 $^{\varepsilon 1}$ A1 test standard, namely the load-displacement curve from which we can calculate the bending stiffness, yield load, yield displacement, bending moment to yield, and bending structural stiffness. The physical and simulated static four-point bending tests of this study resulted in load-displacement curves with excellent concordance as well as agreement between the slopes of the linear elastic regions. Beyond the outputs of a physical test, *Alfonso*™ can also provide 3D visualizations of material failure (e.g., plastic deformation, fracture) as stress and strain field data throughout the entire device during compression. Taken together, this study suggests that *Alfonso*™ can serve as an excellent non-clinical assessment tool in support of pre-regulatory deliberations and regulatory submissions for IMFDs such as humeral nails.

References

[1] ASTM International, "ASTM F1264-16$^{\varepsilon 1}$ Standard Specification and Test Methods for Intramedullary Fixation Devices", doi: 10.1520/f1264-03r12.

[2] J. P. Stannard, H. W. Harris, G. Jr. McGwin, D. A. Volgas, and J. E. Alonso, "Intramedullary Nailing of Humeral Shaft Fractures with a Locking Flexible Nail," *J Bone Joint Surg*, vol. 85, no. 11, pp. 2103–2110, Nov. 2003.

[3] G. M. Schwarz, L. Zak, L. Hirtler, and G. E. Wozasek, "Anatomical considerations of intramedullary humeral nailing and lengthening," *J Clin Med*, vol. 9, no. 3, Mar. 2020, doi: 10.3390/jcm9030806.

[4] A. H. Murdoch, K. J. Mathias, and F. W. Smith, "Measurement of the bony anatomy of the humerus using magnetic resonance imaging," in *Proceedings of the Institution of Mechanical Engineers, Part H: Journal of Engineering in Medicine*, 2002, pp. 31–35. doi: 10.1243/0954411021536252.

[5] M. Niinomi and M. Nakai, "Titanium-based biomaterials for preventing stress shielding between implant devices and bone," *International Journal of Biomaterials*. 2011. doi: 10.1155/2011/836587.

[6] P. Szymczyk-Ziółkowska *et al.*, "Improved quality and functional properties of Ti-6Al-4V ELI alloy for personalized orthopedic implants fabrication with EBM process," *Journal of Manufacturing Process*, vol. 76, pp. 175–194, Apr. 2022, doi: https://doi.org/10.1016/j.jmapro.2022.02.011.

[7] MatWeb, " Titanium Ti-6Al-4V ELI (Grade 23), Annealed," 2023.

[8] AZO Materials, "Grade 23 Ti 6Al 4V ELI Alloy (UNS R56401)," 2013.

[9] Carpenter Technology, "Ti 6Al-4V ELI," Sep. 2021.

[10] L. I.-K. Lin, "A Concordance Correlation Coefficient to Evaluate Reproducibility," *Biometrics*, vol. 45, no. 1, p. 255, Mar. 1989, doi: 10.2307/2532051.

[11] MedCalc Software Ltd, "Concordance correlation coefficient." https://www.medcalc.org/manual/concordance.php (accessed May 27, 2022).

Appendix I

Notes on particle-based method simulation in *Alfonso*™

- "Resolution" (e.g., 50, 200, 500 µm) in *Alfonso*™ is typically equivalent to the diameter of the particles in the model, and thereby the minimum distance within which particles begin to interact. The degree of interaction between particles varies continuously as a function of their distance (e.g., in compression, particles repel more vigorously the closer they are to one another, while the reverse is true for tensile forces acting between "bonded" particles of the same object).
- Each particle represents a small volume of mass of an object in the analysis, the material properties of which (elastic modulus, yield, failure, hardening criteria, etc.) dictate the responses of particles to forces applied during analysis.
- Using the stated material properties from the manufacturer as a starting point, a proprietary scaling factor of the failure mean and standard deviation was applied uniformly to the ultimate strength of Ti-6Al-4V ELI.
- In general, we do not scale material density (i.e., mass) in *Alfonso*™.
- While the initial positions of particles are typically spaced in discrete increments of the resolution (e.g., 200 µm), during analysis particles may continuously move in 3D space. For instance, a particle initially at (200, 200, 200) may move to (200.0034, 199.793403, 202.09809823462) during analysis.
- "Bonds" between particles in *Alfonso*™ are typically formed only at the initial time state, and then only between neighbouring particles of the same object. Bonded particles resist both compression and tension, per the homogeneous or heterogenous properties of the material, until the stress or strain failure limits of the material are exceeded, and a crack is formed. Failed particles remain in analysis (e.g., as debris) and continue to interact with other particles, allowing phenomena such as compaction to be faithfully reproduced in *Alfonso*™.
- "Unbonded" particles that come into contact after analysis has begun (i.e., particles that move to within the minimum distance of interaction) will not form bonds and will only repel one another.
- (See "Beyond FEA: Particle-based simulation 101" at https://www.lifespans.net/publications for further discussion of the basics of mesh-free analysis)